Vacancies and Their Complexes in FCC Metals

L. Yu. Nemirovich-Danchenko, A. G. Lipnitskiĭ, and S. E. Kul'kova

Institute of Strength Physics and Materials Science, Siberian Division, Russian Academy of Sciences, Akademicheskiĭ pr. 2/1, Tomsk, 634021 Russia

e-mail: ndl@ispms.tsc.ru, kulkova@ispms.tsc.ru

Abstract—The formation energies of vacancies and their complexes in copper and nickel at zero and finite temperatures are calculated by the embedded-atom method in the quasi-harmonic approximation. The role of temperature effects in the formation of various atomic configurations of intrinsic point defects is studied.

1. INTRODUCTION

Point defects and their complexes substantially affect the microstructure and its evolution in materials subjected to deformation, hydrogenation, irradiation, and other external influences. For example, the hydrogen saturation of many metals and alloys causes an anomalously large number of vacancies [1], which affects the strength of the material in the technological operations of hydrogen introduction and removal. Increased interest in hydrogen power engineering and hydrogen-accumulating materials requires information on the types of defect complexes in certain materials and their effect on sorption–desorption processes. An important characteristic of defect complexes is their atomic configuration, which is responsible for the defect mobility. A kinetic factor, which results from the formation of primary defects and their structural evolution, is also important. The authors of [2] showed that the kinetics of structural transformations in palladium and its alloys are nonmonotonic: long-term changes in their defect structure were detected. An important kinetic factor is the binding energy of a complex, i.e., the decrease in the free energy of the system induced by the coalescence of point defects to form the complex. The role of this factor increases with the time of system evolution, which develops toward a decrease in the free energy.

The main quantity that controls the atomic structure and size of point-defect complexes (PDCs) is the energy of their formation. Most materials contain a variety of point defects, including vacancies and interstitial and substitutional impurities, and more extended defects, such as dislocations, disclinations, and grain boundaries. Since various types of PDC are simultaneously present in a material, it is difficult to distinguish the effect of defect complexes of a certain type. As a result, it is difficult (or even impossible) to experimentally determine the energy of their formation. The fundamental characteristics of point defects and their complexes are usually obtained from theoretical calculations. Calculating the Gibbs energy of a PDC has recently been reduced to calculating the formation energy at zero temperature [3–6]. However, such calculations ignore the entropy of atomic thermal vibrations, which can substantially affect the Gibbs energy of defects at finite temperatures [7].

In this work, we use model systems (copper, nickel) to calculate the formation and binding energies of vacancies and their complexes at zero and finite temperatures.

2. CALCULATION PROCEDURE

We calculate the Gibbs energy, enthalpy, entropy, and the binding energy of a PDC as a function of temperature using the quasi-harmonic approximation that takes into account the thermal expansion of a crystal lattice. The quantity controlling the PDC stability is the binding energy of the complex, i.e., the difference between the sum of the free Gibbs energies of the single defects forming the complex and the free Gibbs energy of the defect complex. The thermodynamic characteristics of defects are described in terms of excess thermodynamic quantities. An excess thermodynamic quantity ΔX related to a defect is defined to be

$$\Delta X = X_{\text{defect}} - (N_{\text{defect}}/N_{\text{bulk}})X_{\text{bulk}}, \qquad (1)$$

where N_{defect} and N_{bulk} are the numbers of atoms in the system with and without the defect, respectively. The excess thermodynamic quantity related to a defect is determined as the difference between the thermodynamic quantity of the system with the defect and the thermodynamic quantity of the same number of atoms in the volume of the perfect crystal. Then, the excess

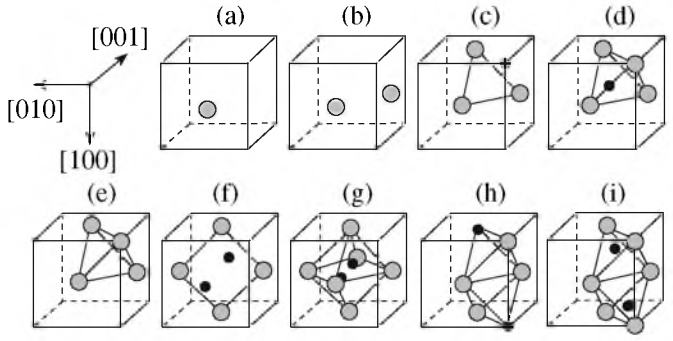

Fig. 1. Point defects and PDCs under study: (a) monovacancy (b) divacancy, (c) planar three-vacancy configuration, (d) tetrahedral three-vacancy configuration, (e) tetrahedral micropore of four vacancies, (f, g) four-vacancy square configuration before (f) and (g) after relaxation, and (h, i) four-vacancy diamond configuration (h) before and (i) after relaxation.

Gibbs free energy of the defect $\Delta G(T)$, or the energy of defect formation, can be written in the form [8]

$$\Delta G(T) = \Delta H(T) - T\Delta S(T) - k_B T \ln g, \qquad (2)$$

where $\Delta H(T)$ and $\Delta S(T)$ are the enthalpy and entropy of the defect, respectively, which are functions of temperature T; g is a geometric factor specifying various types of defects; and k_B is the Boltzmann constant. At zero temperature and zero pressure, the free energy of the defect reduces to the defect-related excess potential energy, which can be calculated by a molecular-statics method for given interatomic potentials. To calculate the enthalpy of the defect at a finite temperature, we average the total energy of the system over a statistical ensemble whose microstates are specified by the Monte Carlo or molecular-dynamics method. The free energy is calculated with more complex theoretical approaches based on thermodynamic integration. In this case, the enthalpy should be preliminarily calculated as a function of temperature [7]. All the methods used for such calculations require high computational capabilities; moreover, their application to even small PDCs is restricted by an insufficient enthalpy calculation accuracy, since energy fluctuations can exceed the energy of defect formation at high temperatures [7]. The computations can be substantially simplified using the quasi-harmonic approximation [9]. With this approach, one can calculate the free energy of a system consisting of several hundred atoms in a calculation cell, which is sufficient for studying small PDCs.

In the quasi-harmonic approximation, the total configuration energy is replaced by a quadratic expansion of the potential energy in atomic displacements near the equilibrium atomic positions at a fixed lattice parameter. Anharmonic effects are taken into account through a change in the lattice parameter. At any value of the lattice parameter, the system is equivalent to a superposition of harmonic oscillators. In the harmonic approximation, the free energy $F(a, T)$ of a solid with a lattice parameter a at a temperature T is

$$F(a,T) = E_0(a) + k_B T \sum_{\mathbf{k},n} \ln\left[2\sinh\left(\frac{\hbar\omega_n(\mathbf{k})}{2k_B T}\right)\right], \qquad (3)$$

where $E_0(a)$ is the energy of the static lattice and $\omega_n(\mathbf{k})$ are the phonon frequencies [10]. Equation (3) describes the free energy as a function of the lattice parameter. At zero pressure, the free energy and volume are calculated by minimizing Eq. (3) with respect to the lattice parameter for each temperature. Other thermodynamic quantities (entropy, enthalpy) can be calculated by taking analogous sums over phonon modes. The calculation procedure is described in more detail in [11]. To specify interatomic potentials, we used the embedded-atom method [12, 13]. Copper and nickel were chosen to be model materials for investigation, since their interatomic potentials are well known [14].

Vacancy complexes in a calculation cell were generated by removing certain atoms from sites of the perfect fcc lattice. The cell size was $a(6 \times 6 \times 6)$, and 864 atoms were in the perfect structure. We also studied smaller ($a(5 \times 5 \times 5)$) and larger ($a(8 \times 8 \times 8)$) cells. The atomic configurations of a PDC were relaxed using the molecular-dynamics method with damping of atom velocities. The relaxation was accompanied by a change in the unit cell volume and was terminated when the force on each atom was smaller than 10^{-4} eV/Å and the pressure did not exceed 10^{-10} GPa. To calculate the thermodynamic quantities in terms of the quasi-harmonic approximation, we need to know the atomic coordinates in a system at a given temperature. In this case, we can also minimize the free energy with respect to the atomic arrangement in the cell [7]. However, this procedure requires the calculation of the third derivatives of the potential energy with respect to atomic displacements, which results in a long computation time in the embedded-atom method. Therefore, the atomic coordinates in the system with a defect were calculated under the assumption that the thermal expansion of the material is uniform; that is, we neglected the difference between the thermal expansion coefficients of the perfect crystal and the defect zone. The atomic coordinates were calculated using the following scheme: (i) the lattice parameter of the perfect crystal was determined at a given temperature in the quasi-harmonic approximation; (ii) the equilibrium positions of atoms in the system with a defect were calculated by minimizing the total energy at zero temperature; and (iii) the obtained atomic coordinates were uniformly changed according to the lattice parameter calculated in the first step. The geometry thus obtained was used to calculate the thermodynamic characteristics of the defect in accordance with the above definition of the excess thermodynamic quantities.

Table 1. Formation energy E_f, volume, and entropy of a monovacancy and divacancy at zero temperature (E_b is the vacancy binding energy)

Defect	E_f, eV	S/k	V_f/V_0	E_b, eV
		Copper		
Monovacancy				
Our calculation	1.27	1.36	0.70	
Other calculations	1.09 [8], 1.11 [16], 1.13 [17]	1.245	0.75 [16]	
	1.21 [5], 1.26, 1.27 [14],	1.404 [14]	0.74, 0.70 [14]	
	1.29 [18], 1.32 [19], 1.33 [20], 1.41 [21]		0.80 [5]	
Experiment	1.03 [22], 1.15 [23], 1.3 [24], 1.17–1.29 [25], 1.28 [26]	2.35 [26]	0.75–0.85 [25]	
Divacancy				0.15
Our calculation	2.39	2.63	1.38	0.15 [27]
Other calculations	2.25 [5], 2.79 [27]		1.63 [5]	0.16 [5]
Experiment	2.15 [23]	7.4 [22]		
		Nickel		
Monovacancy				
Our calculation	1.59	1.95	0.82	
Other calculations	1.51 [16], 1.63 [19], 1.67 [28], 1.77 [17], 1.76 [21]		0.86 [16]	
Experiment	1.6 [29], 1.78 [30], 1.79 [24]		0.97 [31]	
Divacancy				
Our calculation	2.99	3.97	1.59	0.19
Other calculations	3.47 [27]			0.21 [27]

3. GEOMETRY OF POINT-DEFECT COMPLEXES

We considered vacancies and vacancy complexes consisting of at most four point defects. Figure 1 schematically shows the PDCs under study. Apart from a monovacancy and a divacancy (Figs. 1a, 1b), we also analyzed a trivacancy having two possible atomic configurations (Figs. 1c, 1d). In the former case, all vacancies lie in one plane and form an equilateral triangle. In the latter configuration, the atom located at the site that forms a regular tetrahedron together with the three vacancies is shifted to the center of this tetrahedron. This atom is shown as a small solid circle in the initial and final positions in Figs. 1c and 1d, respectively. This configuration represents three vacancies "smeared" over four lattice sites and is a stacking-fault tetrahedron of a minimum size. This configuration was described for the first time in [15]. We also considered three configurations of four-vacancy complexes (tetravacancies). In the first configuration, an atom is removed from the center of a tetrahedron (Fig. 1e) and the complex of four vacancies forms a micropore. In the next configuration, four vacancies are located at the corners of a square. The two small solid atoms in Fig. 1f are relaxed toward the center of the square so that the distance between them becomes $\sim a/\sqrt{2}$. After relaxation, these atoms leave two vacancies behind them and the final configuration consists of six vacancies located at the corners of the octahedron around the displaced atoms (Fig. 1g). The last configuration represents a diamond-type tetravacancy (Fig. 1h). This configuration consists of two equilateral triangles with one common side formed by vacancies. In this case, atoms can shift as in the case considered above for the trivacancy. After relaxation, the atoms tend to occupy the center of the tetrahedron and strongly interact with each other (Fig. 1i).

4. RESULTS AND DISCUSSION

Above all, we discuss the results obtained for vacancy complexes at zero temperature. The results of calculations for the monovacancy and divacancy in copper and nickel are given in Table 1. Copper is one of the most extensively studied materials. Monovacancy formation in copper has been investigated by both semiempirical [5, 8, 14, 16, 28] and ab initio [17–21] methods. As is seen from Table 1, our results agree well with the results of other theoretical calculations and experimental studies. On the whole, the scatter of the calculated values lies within the limits of experimental error. The formation energy of a monovacancy in nickel is higher than that in copper. As follows from the experimental data in [24] and the theoretical calculations in [20] (which were performed with the full-potential linearized muffin-tin orbital (FLMTO) method), the energy of formation of a monovacancy in transition

Table 2. Formation energy E_f, volume, entropy, and binding energy of three- and four-vacancy complexes at zero temperature

Defect	E_f, eV	S/k	V/V_0	E_b, eV
Copper				
Trivacancy, plane	3.38	3.77	2.08	0.44
Trivacancy, tetrahedron	3.41	6.32	1.58	0.40
Tetravacancy, tetrahedron	4.22	3.96	3.05	0.87
Tetravacancy, square	4.35	4.84	2.46	0.73
Tetravacancy, diamond	4.4	5.74	2.69	0.69
Nickel				
Trivacancy, tetrahedron	3.96	9.17	1.94	0.82
Tetravacancy, tetrahedron	5.52	6.06	3.36	0.85
Tetravacancy, square	5.34	11.45	2.70	1.03
Tetravacancy, diamond	4.93	11.89	2.46	1.43

metals increases as the number of d electrons decreases.

Our estimates performed using the full-potential linearized augmented-plane-wave (FLAPW) method in the generalized gradient approximation (GGA) for a cell with 32 atoms with relaxation of the atomic positions and volume show that the energy of vacancy formation in copper is 1.14 eV, which is slightly lower than the value calculated by the above technique and is 0.2 eV lower than the value calculated by the FLMTO method in [20]. It should be noted that the authors of [20] did not take into account relaxation of atomic positions near a vacancy, and the volume of the lattice with a defect was equal to that of the perfect lattice. Moreover, they used the local-density approximation for the exchange–correlation potential.

The divacancy calculations are much scarcer [5]. The energy of divacancy formation agrees well with the value obtained in [5], where the molecular-dynamics and Monte Carlo methods were employed. The difference in the volumetric change induced by the defect formation is more significant (Table 1). The binding energy of vacancies E_b is only 0.01 eV lower than that in [5]. The energy of divacancy formation is somewhat higher than the experimental value (2.15 eV) obtained in [23]. It should be noted that the experimental value was obtained for monovacancies or monovacancies along with divacancies. The calculated energy of monovacancy formation in nickel also agrees satisfactorily with the experimental data. The binding energy of vacancies in nickel is only slightly higher than in copper.

In the literature, it is assumed [32] that it is the tetrahedral configuration of a trivacancy (which is virtually immobile) that serves as a nucleation center for pore growth in materials. The nucleation center can grow via joining a fourth vacancy. It is generally accepted that a large number of excess vacancies do not directly join to form a pore due to the exponentially decreased probability of a large number of vacancies meeting together. On the other hand, a trivacancy in the planar configuration has a low migration energy [32] and can rapidly reach sinks at high temperatures. Therefore, it is interesting to understand the physical nature of the formation of a certain defect configuration.

Table 2 lists the formation energies of the PDCs consisting of three or four vacancies and having the above configurations. We will discuss the calculation results for groups of complexes of the same size. Our calculations demonstrate that the planar configuration of a trivacancy in copper is energetically favorable. However, the difference in the energies of this configuration and the tetrahedral configuration is rather small (~0.03 eV). The calculations in [15] predicted the stability of a trivacancy in the form of a tetrahedron, whereas in [32] the planar configuration was found to be stable. Note that the tetrahedral configuration of a trivacancy proved more stable in nickel at zero temperature. Among the four-vacancy complexes in copper, the complex with a tetrahedral configuration (micropore) is most stable (Table 2). In nickel, the diamond-type four-vacancy complex is energetically favorable (Fig. 1h). In this case, the energy of formation of this configuration is 0.59 eV lower than that of the tetrahedral configuration. In copper, the difference between the energies of these configurations is 0.18 eV. Moreover, the energy of the square vacancy complex formation in copper differs only slightly (by ~0.05 eV) from the energy of the diamond-type PDC.

The temperature dependences of the energy of formation and binding energy of PDCs in copper and nickel are shown in Figs. 2 and 3. We do not present the temperature dependences of the formation energies of mono- and divacancies in these figures, since these energies vary with temperature only slightly in both nickel and copper (which agrees with the results from [28]). For example, the energy of monovacancy formation in copper at 800 K is 1.177 eV (1.181 eV [28]). As was found in [28], the energy of monovacancy formation in copper changes from 1.25 to 1.15 eV over the temperature range from 0 to 1000 K. The calculated thermodynamic quantities (enthalpy, entropy) are also consistent with the results from [28]. Our results also agree with the data from [28] on the temperature dependences obtained for nickel. The energy of monovacancy formation in nickel at a $T = 800$ K is 1.467 eV (1.503 eV [28]). The enthalpy and entropy of divacancy formation in copper obtained in [8] (2.33 and 2.84 eV, respectively) are consistent with our results (2.38 and 2.63 eV, respectively). Unfortunately, there are no published data on the temperature dependences for vacancy complexes. Our calculations show that, as the temperature increases above 150 K, the tetrahedral configuration of a trivacancy becomes more stable than the planar configuration (Fig. 2). As is seen from Fig. 2, the binding energy of a trivacancy in the tetrahedral

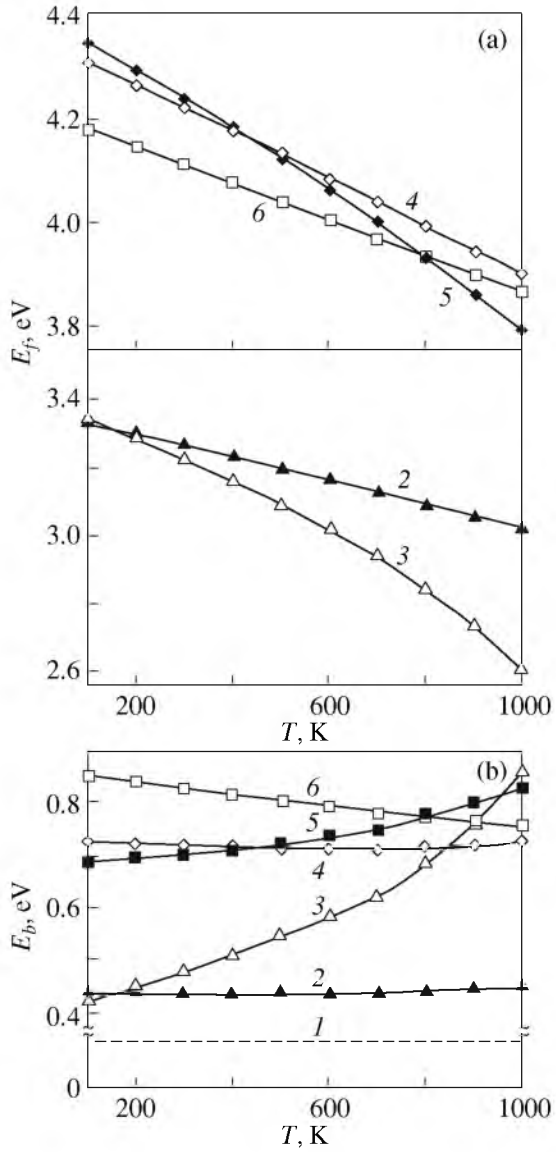

Fig. 2. (a) Formation and (b) binding energies of vacancy complexes as functions of temperature in copper: (*1*) divacancy, (*2*) planar trivacancy, (*3*) tetrahedral trivacancy, (*4*) diamond-type tetravacancy, (*5*) square tetravacancy, and (*6*) tetrahedral tetravacancy.

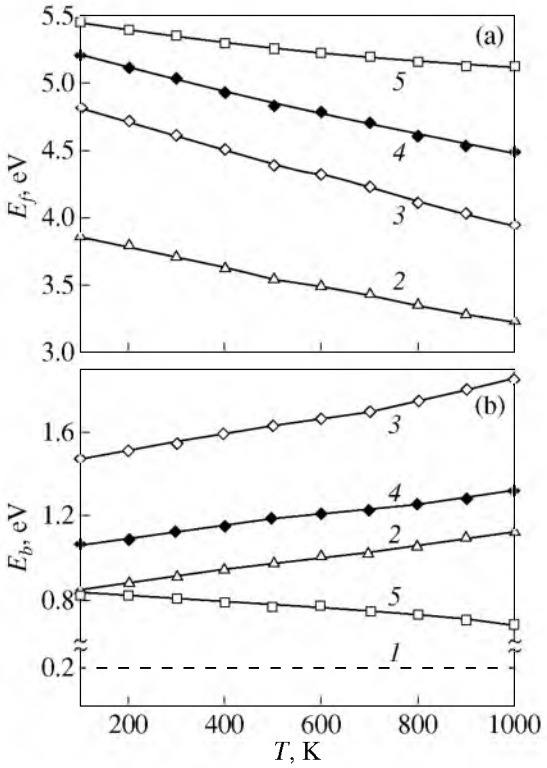

Fig. 3. (a) Formation and (b) binding energies of vacancy complexes as functions of temperature in nickel: (*1*) divacancy, (*2*) tetrahedral trivacancy, (*3*) diamond-type tetravacancy, (*4*) square tetravacancy, and (*5*) tetrahedral tetravacancy.

configuration increases rapidly with temperature, whereas its formation energy decreases. At 800 K, this difference is 0.26 eV.

Figure 4 shows the calculated contributions of atomic thermal vibrations to the entropy of formation of the two trivacancy configurations in copper. The entropy of a trivacancy in the tetrahedral configuration substantially exceeds the entropy of the planar configuration and increases with temperature. This behavior also explains the strong temperature dependence of the binding energy of the tetrahedral trivacancy, since the enthalpy of PDC formation is virtually independent of temperature [11]. The relatively high values of the entropy of the trivacancy are caused by the specific features of its atomic configuration. The atom at the center of the tetrahedron formed by vacant sites (Fig. 1d) weakly interacts with the other atoms of the crystal lattice, which causes low frequencies of its thermal vibrations and a large contribution of the tetrahedral trivacancy to the excess entropy. The entropy of thermal vibrations increases with the vibrational density of states at low frequencies. As a result of the thermal expansion of the lattice, the interaction of the atom in the tetrahedron with the other lattice atoms weakens, which leads to an additional increase in the trivacancy entropy. The potential barrier between the tetrahedral and planar trivacancy configurations is small (0.024 eV at 0 K). Therefore, as the temperature increases, the atom at the center of the tetrahedron is in a flatter effective potential as compared to the parabolic potential of the quasi-harmonic approximation. Note that the variations with temperature observed in copper are also observed for divacancy formation in nickel. The decrease in the energy of trivacancy formation with increasing temperature in nickel is also pronounced (Fig. 3a). As noted above, the minimum energy of tetravacancy formation in copper is characteristic of the tetrahedral configuration (micropore); however, as the temperature increases, the square configuration

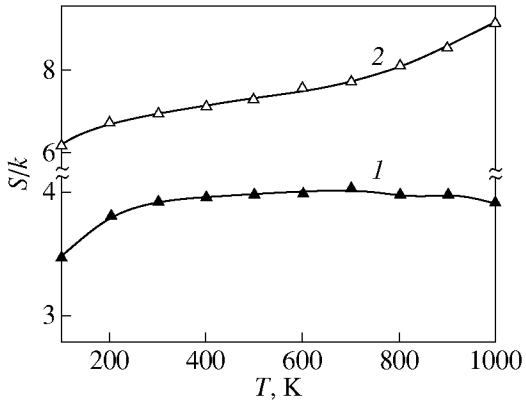

Fig. 4. Temperature dependence of the entropy of a vacancy complex in copper: (*1*) planar trivacancy and (*2*) tetrahedral trivacancy.

becomes more stable. The energies of these two types of vacancy complexes (square and diamond) differ insignificantly up to 600 K. Therefore, other factors, including impurities, can substantially affect the stability of tetravacancies in copper. The obtained results indicate that the addition of a fourth vacancy to form a micropore is energetically favorable only below a critical temperature (about 900 K) at which the binding energy of the tetrahedral trivacancy coincides with the binding energy of the micropore. This conclusion agrees qualitatively with the results of investigating the high-temperature coalescence of excess vacancies in fcc metals [33, 34].

Among the four-vacancy complexes in nickel, the diamond-type vacancy complex has a minimum formation energy. This complex remains energetically favorable at all temperatures under study, and this thermodynamic preference increases with temperature. The temperature dependences of the entropies of all four-vacancy configurations except for the diamond-type configuration are found to be weak, which indicates that they do not have specific features inherent in the atomic structures of the trivacancy configurations. It is interesting that, in nickel, the entropy contributions of all four-vacancy complexes increase in the temperature range 100–600 K and then level off. As is seen from Fig. 3b, the binding energies of all vacancy complexes in nickel (except for the micropore configuration) increase with temperature. The formation of the tetrahedral configuration of a trivacancy becomes energetically more favorable with increasing temperature.

5. CONCLUSIONS

We have calculated the thermodynamic characteristics of single vacancies and their complexes in the quasi-harmonic approximation using interatomic potentials constructed by the embedded-atom method. The calculated energies and volumes of formation of these defects at zero temperature agree satisfactorily with the results of other theoretical calculations and experimental studies. The thermodynamic characteristics of point-defect complexes at finite temperatures have been calculated. The stabilization of the tetrahedral configuration of a trivacancy in copper has been shown to be mainly caused by the entropy due to atomic thermal vibrations. The entropy of formation of the tetrahedral configuration of a trivacancy in copper is significantly higher than that of its planar configuration, and this difference increases with temperature. However, the formation of a four-vacancy complex (micropore) in copper is thermodynamically more favorable only up to a critical temperature of about 900 K; at higher temperatures, excess vacancies can coalesce. The energies of formation of four-vacancy complexes in copper differ insignificantly over the entire temperature range under study. In nickel, the binding energy of vacancies in a diamond-type configuration is significantly higher than that in the other vacancy complexes over the entire temperature range.

ACKNOWLEDGMENTS

This work was supported by the Russian Foundation for Basic Research, project nos. 04-02-39009 GFEN_2004a and 04-02-17221a.

REFERENCES

1. V. M. Avdyukhina, A. A. Anishchenko, A. A. Katsnel'son, and G. P. Revkevich, Perspekt. Mater., No. 4, 5 (2002).
2. V. M. Avdyukhina, A. A. Katsnel'son, and G. P. Revkevich, Kristallografiya **44** (1), 49 (1999) [Crystallogr. Rep. **44** (1), 44 (1999)].
3. P. Zhao and Y. Shimomura, Comput. Mater. Sci. **14**, 84 (1999).
4. N. Tajima, O. Takai, Y. Kogure, and M. Doyama, Comput. Mater. Sci. **14**, 152 (1999).
5. H. Deng and D. J. Bacon, Phys. Rev. B: Condens. Matter **48**, 10022 (1993).
6. K. J. Morishita, J. Nucl. Mater. **283–287**, 753 (2000).
7. S. M. Foiles, Phys. Rev. B: Condens. Matter **49**, 14930 (1994).
8. N. Sandberg and G. Grimvall, Phys. Rev. B: Condens. Matter **63**, 184109 (2001).
9. K. A. Putilov, Thermodynamics (Nauka, Moscow, 1971) [in Russian].
10. N. Ashcroft and N. Mermin, *Solid State Physics* (Holt, Rinehart and Winston, 1976; Mir, Moscow, 1979), Vol. 2.
11. A. G. Lipnitskiĭ, S. D. Borisova, I. P. Chernov, and L. Yu. Zagorskaya, Fiz. Mezomekh. **6**, 93 (2003).
12. M. S. Daw and M. I. Baskes, Phys. Rev. Lett. **50**, 1285 (1983).
13. M. S. Daw and M. I. Baskes, Phys. Rev. B: Condens. Matter **29**, 6443 (1984).
14. Y. Mishin, Phys. Rev. B: Condens. Matter **63**, 224106 (2001).

15. A. C. Damask, G. J. Dienes, and V. G. Weizer, Phys. Rev. **113**, 781 (1959).
16. J.-E. Kluin, Philos. Mag. A **65**, 1263 (1992).
17. T. Hoshino, N. Papanikolaou, R. Zeller, P. H. Dederichs, M. Asato, T. Asada, and N. Stefanou, Comput. Mater. Sci. **14**, 56 (1999).
18. B.-J. Lee, J.-H. Shim, and M. I. Baskes, Phys. Rev. B: Condens. Matter **68**, 144112 (2003).
19. S. V. Eremeev, A. G. Lipnitskiĭ, A. I. Potekaev, and E. V. Chulkov, Izv. Vyssh. Uchebn. Zaved., Fiz., No. 3, 62 (1997).
20. T. Korhonen, M.J. Puska, and R. M. Nieminen, Phys. Rev. B: Condens. Matter **51**, 9526 (1995).
21. H. M. Polatoglou, M. Methfesseel, and M. Scheffler, Phys. Rev. B: Condens. Matter **48**, 1877 (1993).
22. B. Drittler, M. Weinert, R. Zeller, and P. H. Dederichs, Solid State Commun. **79**, 31 (1991).
23. G. J. Ackland, G. Tichy, V. Vitek, and M. W. Finnis, Philos. Mag. A **56**, 735 (1987).
24. P. Ehrhart, P. Jung, H. Schultz, and H. Ullmaier, in *Landolt–Börnstein Numerical Data and Functional Relationships in Science and Technology, New Series*: *Group III. Crystal and Solid State Physics* (Springer, Berlin, 1991).
25. R. W. Balluffi, J. Nucl. Mater. **69–70**, 240 (1978).
26. W. Schule, Z. Metallkd. **89**, 672 (1998).
27. S. V. Eremeev, A. G. Lipnitskiĭ, A. I. Potekaev, and E. V. Chulkov, Izv. Vyssh. Uchebn. Zaved., Fiz., No. 6, 83 (1997).
28. L. Zhao, R. Najafabadi, and D. J. Srolovitz, Modell. Simul. Mater. Sci. Eng. **1**, 539 (1993).
29. W. Wycisk and M. Feller-Kniepmeier, J. Nucl. Mater. **69–70**, 616 (1978).
30. O. Bender and P. Ehrhart, *Point Defects and Defect Interactions in Metals* (North-Holland, Amsterdam, 1982), p. 639.
31. H.-E. Schaefer, Phys. Status Solidi A **102**, 47 (1987).
32. I. I. Novikov, *Defects of the Crystalline Structure of Metals* (Metallurgiya, Moscow, 1983) [in Russian].
33. Yu. N. Osetsky and D. J. Bacon, Nucl. Instrum. Methods Phys. Res., Sect B **202**, 31 (2003).
34. Yu. N. Osetsky and D. J. Bacon, Nucl. Instrum. Methods Phys. Res., Sect. B **180**, 85 (2001).

Translated by K. Shakhlevich